

# The Impact of an Oxygen Dopant in an ideal $\text{Bi}_2\text{Sr}_2\text{CaCu}_2\text{O}_{8+\delta}$ Crystal

S. Johnston<sup>1,2</sup>, F. Vernay<sup>3</sup>, and T.P. Devereaux<sup>2</sup>

<sup>1</sup>*Department of Physics, University of Waterloo, Waterloo, Ontario, N2L 3G1, Canada*

<sup>2</sup>*Department of Photon Science, Stanford Linear Accelerator Center,  
Stanford University, Menlo Park, CA, 94025, USA and*

<sup>3</sup>*Paul Scherrer Institut, Condensed Matter Theory Group, Villigen PSI, Switzerland*

(Dated: September 17, 2008)

Recent scanning tunneling microscopy studies have shown that local nanoscale pairing inhomogeneities are correlated with interstitial oxygen dopants in  $\text{Bi}_2\text{Sr}_2\text{CaCu}_2\text{O}_{8+\delta}$ . Combining electrostatic and cluster calculations, in this paper the impact of a dopant on the local Madelung and charge transfer energies, magnetic exchange  $J$ , Zhang-Rice mobility, and interactions with the lattice is investigated. It is found that electrostatic modifications locally increases the charge transfer energy and slightly suppresses  $J$ . It is further shown that coupling to  $c$ -axis phonons is strongly modified near the dopant. The combined effects of electrostatic modifications and coupling to the lattice yield broadened spectral features, reduced charge gap energies, and a sizable local increase of  $J$ . This implies a strong local interplay between antiferromagnetism, polarons, and superconducting pairing.

The precise role of the atoms lying off the  $\text{CuO}_2$  planes has been an intriguing puzzle in the cuprates. While largely thought to provide a charge reservoir to dope holes into the  $\text{CuO}_2$  plane, it has become clear that an understanding of the pairing mechanism will require addressing the large variations in  $T_c$  arising from the local environment surrounding the  $\text{CuO}_2$  planes[1]. Empirically, the role of the apical or axial orbitals has been a vehicle linking  $T_c$  to either an effective electron hopping  $t'$  along diagonal Cu-Cu bonds[2], or to the stability of the Zhang-Rice singlet (ZRS)[3]. However to date these arguments have pointed out possible links but offer little microscopic reason for the impact on  $T_c$  itself.

Scanning tunneling microscopy (STM) in  $\text{Bi}_2\text{Sr}_2\text{CaCu}_2\text{O}_{8+\delta}$  (Bi2212) has revealed that nanoscopic inhomogeneity is correlated with the location of interstitial oxygen dopant atoms[4] or the superlattice modulation[5]. The location of dopants has been correlated with suppressed peak features with larger gap energies in the observed local density of states (LDOS), and have been associated with local modification of superconducting pairing[6]. This suggests a non-trivial link between the dopant atoms and the electronic properties of the material on a local level.

In metallic systems, such defects can be effectively screened and have little impact on the electrostatics of the material. This is in contrast to the cuprates, which have poor screening along the  $c$ -axis and are unable to effectively screen the dopant's impurity charge. As a result, these dopants and accompanying structural changes may have a substantial impact on the electrostatic properties of the material. This may be reflected in quantities such as the charge transfer energy  $\Delta$ , effective hoppings  $t, t'$ , magnetic exchange interaction  $J$ , or electron-phonon (el-ph) coupling strength  $\lambda$ .

From  $t - J$  studies[7], it has been argued that dopants give an enhancement of  $J$  and thus larger gap energies,

yet the overall shape of the LDOS suggests that incoherence, giving broad spectral features, is an important ingredient to understand local pairing modifications.

In order to quantitatively address these issues electrostatic Ewald calculations are performed for Bi2212 supercells to determine the spatial dependence of the Madelung energies around atomic sites in the crystal. It is found that while Madelung energies on O and Cu are spatially varied on the scale of eVs, these changes largely cancel and  $\Delta$  is slightly increased near the dopant, yielding an overall suppression locally to  $J$ . This information is then combined into exact diagonalization (ED) cluster studies, yielding effective parameters  $t, t', J$  and  $J'$ . Large  $O(1)$  changes are found both in  $t'$  as well as  $c$ -axis el-ph coupling  $\lambda$ , quantities which are known to strongly modify a  $d_{x^2-y^2}$  pairing interaction. Finally ED cluster studies including  $c$ -axis phonons are shown to produce broadened spectra, a reduced charge gap, in agreement with experiments[4]. As a consequence, a sizable local increase of  $J$  results due to reduced gap via a gain in lattice energy, implying a strong interplay between el-ph coupling, and local superconducting pairing and antiferromagnetic correlations.

Electrostatic calculations using Ewald's method are performed on a supercell consisting of  $3 \times 3 \times 1$  Bi2212 unit cells and containing 270 atoms. We have examined supercells up to four times this size and found that the results are not qualitatively different. Each unit cell contains 2-primitive cells stacked along the  $c$ -axis for a total of 4  $\text{CuO}_2$  planes, as shown in Fig. 1a. Using formal valences for the atoms along with the known structural data[8], the Madelung energies  $\Phi$  obtained are  $\Phi_{\text{apex,plane}} = 18.48, 10.16$  eV for the apical, planar oxygen sites respectively, and  $\Phi_{\text{Cu}} = -38.22$  eV for the copper site, consistent with values reported previously[3]. The charge transfer  $\Delta$  is related to the difference in Madelung energies for the Cu and O sites,

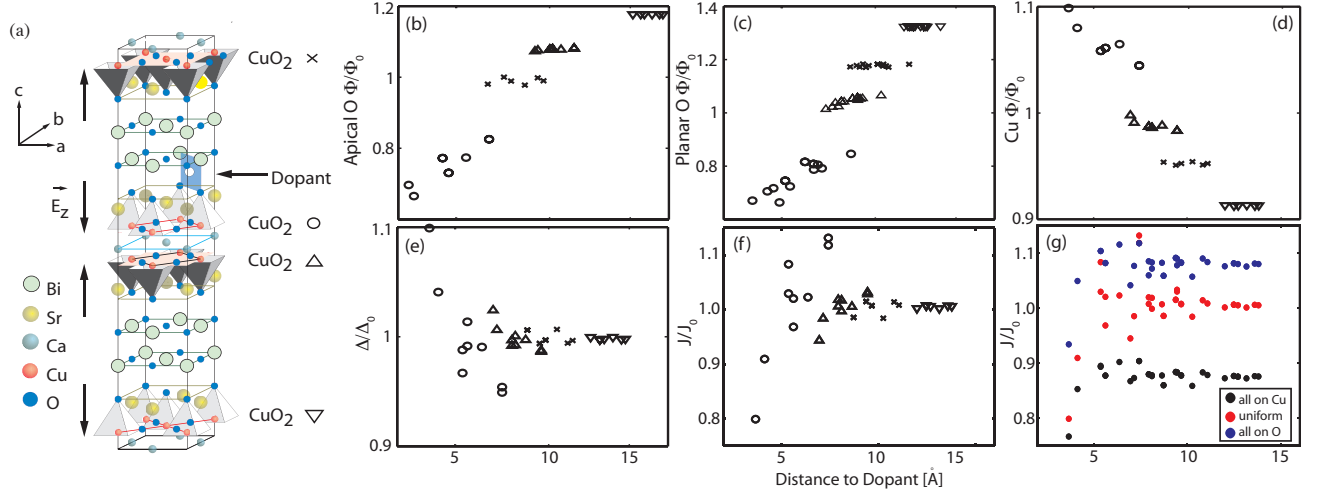


FIG. 1: (a) Schematic location of the dopant oxygen in Bi-2212 unit cell. Individual CuO<sub>2</sub> planes are labeled by the symbols shown. The arrows on the left indicate the orientation of the local oxygen crystal fields for the undoped lattice. (b - d) Madelung energies of the apical O, planar O and Cu sites, respectively, in the doped lattice. The local value of the charge transfer energy  $\Delta$  (e) and derived exchange interaction  $J$  (f), obtained by averaging  $\Delta\Phi_M$  between Cu and its four neighbouring O sites. (g) Resulting  $J$  for different distributions of charges. All values have been normalized to the undoped lattice values. The distance to dopant is defined as the distance to the closest dopant, accounting for the periodicity of the superlattice.

$\Delta\Phi_M = \Phi_O - \Phi_{Cu}$  and is given by:

$$\Delta = \frac{\Delta\Phi_M}{\epsilon(\infty)} - I_{Cu}(2) + A_O(2) - \frac{e^2}{d_p} \quad (1)$$

where  $I_{Cu}(2)$  and  $A_O(2)$  are the second ionization and electron affinity energies for the Cu and O sites respectively. The factor of  $e^2/d$  represents the contribution of the Coulomb interaction between the introduced electron-hole pair. In this work we take the dielectric constant  $\epsilon(\infty) = 3.5$  and  $I_{Cu}(2) - A_O(2) + e^2/d = 10.9$  eV[3], yielding  $\Delta = 2.92$  eV. Besides setting the energy scale for gap excitations,  $\Delta$  largely governs the magnetic exchange energy  $J$ . Using a canonical standard set of parameters in the limit of small hole hopping[9, 10], an exchange energy  $J \sim 300$  meV is obtained. This value larger than that found in experiments[11] results from the limitations of a perturbative expression for experimentally relevant parameter sets.

The Ewald calculation was then repeated with a single oxygen dopant atom inserted into the unit cell, shown schematically in Fig. 1a, and the neighbouring atoms displaced as indicated from recent LDA studies[12]. The oxygen dopant was assigned formal valence, with surplus charge distributed equally among orbitals in the closest CuO<sub>2</sub> planes.

The site-dependent Madelung energies are presented in Fig. 1b-d, showing large scale variations for sites closest to the dopant atom. Suppressions/enhancements of O/Cu Madelung energies are observed, respectively, rising/falling to bulk values, shifted by the presence of doped holes, further away from the dopant. However,

since the relative sign of the Madelung energies for Cu & O are negative, these changes largely cancel for  $\Delta\Phi_M$  and thus  $\Delta$  (Fig. 1e) is largely unaffected.

Modifications in  $\Delta$  allow us to examine the effect of the dopant on the exchange energy  $J$  (Fig. 1f). Reflecting the spatial variations of  $\Delta$ ,  $J$  is suppressed by up to 20 % near the dopant. Allocating dopant excess charge on either on Cu, on O, or distributed on both result in slightly different values of  $J$  (Fig. 1g) but the overall suppression seems rather immune to the way in which charge is distributed.

To test this in a non-perturbative way ED studies of three-hole Cu<sub>2</sub>O<sub>7</sub> (Fig. 2a) and Cu<sub>2</sub>O<sub>8</sub> (Figs. 2b & 2c) clusters were employed to determine changes to the ZRS parameters[13]. Including Cu  $3d_{x^2-y^2}$ , O  $2p_x$  and  $2p_y$  orbitals, the Hamiltonian is  $H = \sum_{i,\sigma} H_{i,\sigma}$  where:

$$\begin{aligned} H_{i,\sigma} = & \epsilon_d^i d_{i,\sigma}^\dagger d_{i,\sigma} + \sum_{\delta} \epsilon_p^{i,\delta} p_{i,\delta,\sigma}^\dagger p_{i,\delta,\sigma} \\ & + \sum_{\delta} t_{pd}^{i,\delta} [d_{i,\sigma}^\dagger p_{i,\delta,\sigma} + h.c.] + \sum_{\delta,\delta'} t_{pp}^{\delta,\delta'} p_{i,\delta,\sigma}^\dagger p_{i,\delta',\sigma} \\ & + U_{dd} \hat{n}_{i,\uparrow} \hat{n}_{i,\downarrow} + U_{pp} \sum_{\delta} \hat{n}_{i,\delta,\uparrow} \hat{n}_{i,\delta,\downarrow} \end{aligned} \quad (2)$$

where  $\delta$  denotes the Cu-O basis vectors and  $\hat{n}$  the number operator. From this 3-band model, an effective single-band Hubbard or  $t - J$  model is derived, with effective nearest  $2t$  and next-nearest  $2t'$  neighbour hoppings determined from the bonding/anti-bonding splitting of the ZRS, and  $J$  derived from singlet-triplet splitting. In terms of clusters Cu<sub>2</sub>O<sub>7</sub> determines  $t$  and  $J$  as the ZRS involves a common bridging oxygen while Cu<sub>2</sub>O<sub>8</sub> clusters

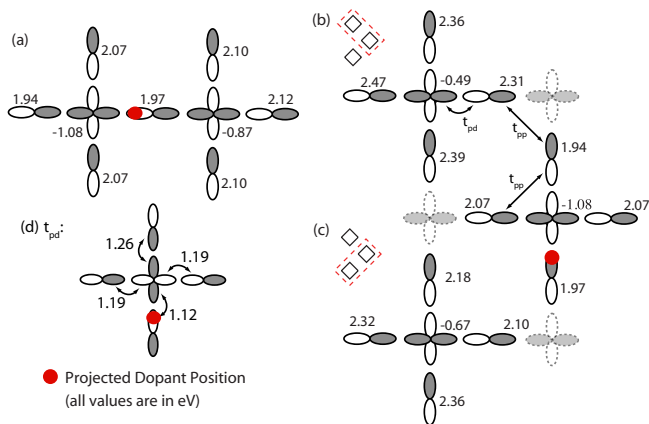


FIG. 2: (a)  $\text{Cu}_2\text{O}_7$  cluster used to extract  $t$  and  $J$ . (b) and (c) Two  $\text{Cu}_2\text{O}_8$  clusters shown in red outline used to extract  $t'$  and  $J'$ . The values for  $\epsilon_{p,d}$  are indicated. (d) modifications to  $t_{pd}$  due to the dopant induced displacements.

yield  $t'$ ,  $J'$  via O-O hopping[13]. For the undoped lattice,  $t = 383$ ,  $t' = -141$  meV and antiferromagnetic exchange couplings of  $J = 218$ ,  $J' = 17$  meV are characteristically obtained.  $J$  may be fine-tuned by adjusting  $t_{pd}$  and  $t_{pp}$ .

The dopant is included by locally varying the on-site Cu and O energies  $\epsilon_d$  and  $\epsilon_p$ , respectively, shown in Fig. 2. Here two  $\text{Cu}_2\text{O}_8$  clusters are used which differ with respect to the location of the dopant, and the site energies have been determined from site modified Madelung energies (Fig. 1), according to Eq. 1. For the  $\text{Cu}_2\text{O}_7$  cluster  $t = 390$ ,  $J = 216$  meV are obtained, while for the two  $\text{Cu}_2\text{O}_8$  clusters (Figs. 2b & 2c) we obtain  $t' = -242(-189)$  meV and  $J' = 18(17)$ , respectively. Electrostatic modifications to  $J$  and  $J'$  are slightly suppressed over undoped cluster values, in general agreement with Madelung estimates, although the magnitude is smaller. Importantly, we note that the symmetric placement of the dopant for the  $\text{Cu}_2\text{O}_7$  cluster gives only small changes to  $t$ , while for  $\text{Cu}_2\text{O}_8$  the increases are noticeably larger, particularly for geometry Fig. 2b compared to 2c. The asymmetric location of the dopant favors occupation of the oxygen ligand orbitals in the plaquette containing the dopant, giving larger modification of  $t'$ .

We have repeated these cluster calculations, including the modulations in  $t_{pd}$  induced by the structural distortions, according to the LDA displacements of Cu-O bond-distances[12, 14], shown in Fig. 2d, and obtain  $t = 374$ ,  $J = 197$ ,  $t' = -231(-180)$  and  $J' = 17(16)$  meV. This tends to further suppress  $J$ . Thus oxygen dopant's net effect is to mildly suppress  $J$  and increase  $t'$ , indicating that the dopant cannot be viewed as only modifying site energies and increasing  $J$  in downfolded single band models[7].

Since the Madelung energies are locally modified on the eV scale, real space modifications may result in sub-

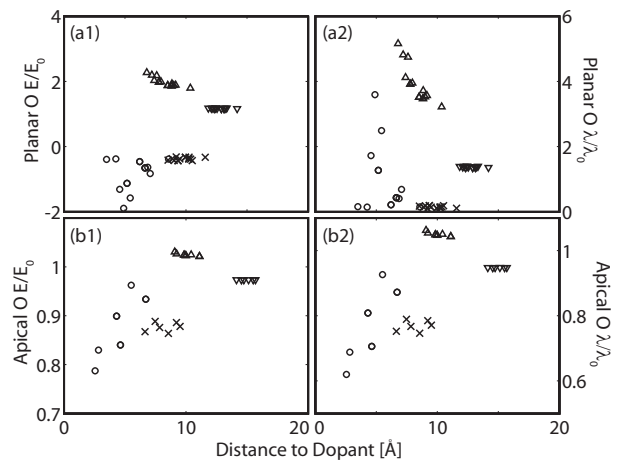


FIG. 3: (a1), (b1) Normalized local crystal fields at the planar and apical oxygen sites of the doped lattice. (a2), (b2) The corresponding electron phonon coupling strength  $\lambda \propto E^2$ . The data points follow the same key as figure 1.

stantial changes to local crystal fields. Ions vibrating along the  $c$ -axis are sensitive to spatial gradients of the Madelung energies, and Ref. 15 has shown that these values of the local field determines the overall strength of el-ph coupling at the oxygen sites, controlling coupling to Raman active  $A_{1g}$  planar and apical oxygen vibrations, and out-of-phase planar  $B_{1g}$  vibrations. Therefore, we have examined the dopant's effect on the crystal field in connection to local changes in el-ph coupling.

For the undoped crystal,  $c$ -axis crystal fields are  $E_{apex,plane} = 18.74, 1.16$  eV/Å for the apical, planar oxygen sites, respectively, oriented as indicated in Fig. 1a. For the doped lattice, in Figs. 3a1, b1 we plot the local  $c$ -axis electric field strength at the planar, apical oxygen sites, respectively, and the corresponding el-ph coupling strength  $\lambda$  in Figs. 3a2, b2[15]. One can see that the  $E$ -field strength is very sensitive to the local symmetry breaking introduced by the dopant, especially in the case of the planar oxygen atoms. The presence of the dopant's bare charge in the otherwise positively charged SrO/BiO structure suppresses the field in the closest lying plane and the structural changes further modify the local fields. The largest changes to the  $E$ -field occur in the plane whose field is oriented towards the dopant. In this case the geometry is such that the dopant's bare charge increases the strength of the original field, driving  $\lambda$  for the  $c$ -axis planar oxygen modes up by a factor of 5. As it is well known that the  $c$ -axis phonons give an attractive interaction in the  $d_{x^2-y^2}$  channel, this suggests that superconductivity may be locally promoted by the dopant, in agreement with the assessment of Ref. 6. The enhanced el-ph coupling may on the otherhand drive a tendency to locally bind a hole to the lattice near the dopant location. This raises the possibility that LDOS modifications could be related to local polarons rather

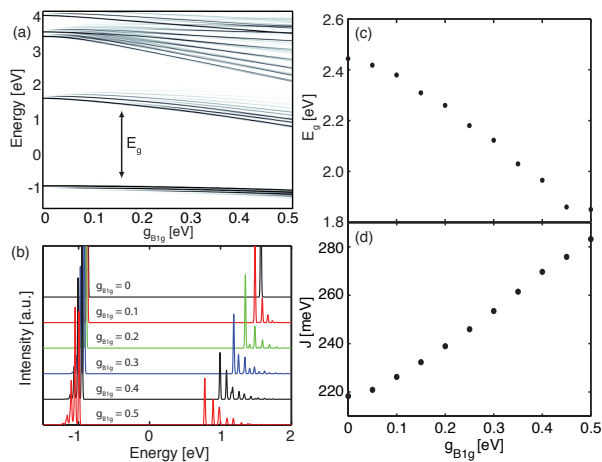


FIG. 4: (a) The electron addition and removal spectra for the  $\text{CuO}_2$  cluster coupled to  $c$ -axis oxygen vibrations as a function of el-ph coupling strength. The energy gap  $E_g$  is indicated. (b) The electron addition (positive energy) and removal (negative) spectra as a function of energy for selected coupling strengths. (c,d)  $E_g$ ,  $J$  as a function of el-ph coupling, respectively.

than pairing.

To address this issue, we examine three-site polarons via ED for an isolated  $\text{CuO}_2$  Hubbard cluster coupled to  $c$ -axis oxygen vibrations:  $H = H_{el} + H_{lat} + H_{el-ph}$ , where  $H_{el}$  is defined in Eq. 2, and  $H_{lat} = \sum_{\nu} \Omega_{\nu} \hat{n}_{\nu}$ ,  $H_{el-ph} = \sum_{\nu, \delta, \sigma} g_{\nu} (b_{\nu}^{\dagger} + b_{\nu}) e_{\nu}^{\delta} p_{\delta, \sigma}^{\dagger} p_{\delta, \sigma}$ . Here  $\hat{n}_{\nu}$  is the phonon-number operator for branch  $\nu$ ,  $e_{\nu}^{\delta}$  is the polarization of the  $\nu$ -th quantized local displacement, and  $g_{\nu} = eE\sqrt{\hbar/2M_O\Omega_{\nu}}$  sets the el-ph coupling strength to mode  $\nu$ . We consider coupling to uniform out-of-phase  $B_{1g}$  and in-phase  $A_{1g}$   $c$ -axis modes ( $\Omega = 36$  and  $55$  meV, respectively) coupled to the oxygen hole density by the local field  $eE$ . We have not included any local modifications to the phonon mode energies compared to the bulk.

To make contact to STM LDOS, the electron addition, removal spectra  $A_{\pm}$ , defined as

$$A_{\pm}(\omega) = \sum_i |\langle \Psi_i^{0,2} | c, c^{\dagger} | \Psi_{gs}^1 \rangle|^2 \delta(\omega - E_i^{0,2} + E_{gs}^1), \quad (3)$$

where  $\Psi_i^n$  denotes the  $n$ -hole states with energy  $E_i^n$ , are plotted in Figs. 4a & 4b for different values of el-ph coupling  $g_{B_{1g}}$ . A large number of phonon quanta have been used such that the results are independent of the number of phonons for the parameter region investigated. As the coupling is increased, the spectral weight is gradually transferred into phonon side bands giving broader and suppressed spectral peaks. The corresponding energy gap  $E_g$  between the first removal and addition states decreases with increasing  $g_{B_{1g}}$  (Fig. 4c) as the effective charge transfer energy is reduced by the gain in lattice energy. As a consequence, the value of  $J$  (correspondingly

determined from 2-hole  $\text{Cu}_2\text{O}_7$  clusters with phonons) increases substantially with increasing  $g_{B_{1g}}$ , as shown in Fig. 4d. The decrease of  $E_g$  and increase of  $J$  due to local phonons will overwhelm the countering effects from purely electrostatic considerations as the coupling to the lattice increases.

To estimate the size of the effect for Bi-2212,  $E_{plane} = 1.16$  eV for the undoped lattice yields  $g_{B_{1g}} \sim 0.073$  eV, well into the large polaron regime where side-bands are weak. Near the dopant however  $g_{B_{1g}}$  is enhanced to  $\sim 0.2$  eV, where side bands begin to develop spectral weight in the removal/addition spectra and the charge gap is reduced (Figs. 4a-c). At the same time, for this parameter regime, which is characteristic of multilayer cuprates,  $J$  is increased by 20 meV. much greater than the small reduction determined from electrostatic effects alone. Thus for realistic parameter regimes,  $c$ -axis phonons act in concert with strong spatial variations of Madelung energies give an increase in  $J$  as well. The dopant may then provide two coupled channels for  $d$ -wave pair enhancement, while causing suppressed spectral features as a consequence of strong local e-ph coupling. This is qualitatively what has been observed in experiments[4]. Such synergy between phonons, polarons and antiferromagnetism has been already noticed in cluster quantum Monte Carlo studies[16].

In summary, we have investigated electrostatic modulations of local Madelung energies arising from the presence of a dopant atom in Bi-2212 unit cells. While eV changes are found for the Madelung energies for copper and oxygen, these changes largely cancel for the charge transfer energy and give small local suppression to  $J$ . However the strong local variations in Madelung energies are manifest in order 1 changes in el-ph coupling for  $c$ -axis oxygen modes. Using cluster studies, it was found that in combination electrostatic modifications and coupling to the lattice yield broadened spectral features, reduced charge gap energies  $E_g$ , and a sizable local increase of  $J$ , implying a strong local interplay between antiferromagnetism, polarons, and superconducting pairing. The amount of variation of the local charge gap can thus serve as an important diagnostic for determining lattice coupling, electrostatic effects, and pairing. It is an open question whether a link between these quantities can be made experimentally.

The authors would like to acknowledge valuable discussions with A. Balatsky, J. C. Davis, W. Harrison, P. J. Hirschfeld, H.-P. Cheng, K. McElroy, B. Moritz, and J.-X. Zhu. This work was supported by NSERC.

- 
- [1] H. Eisaki *et al.*, Phys. Rev. B **69**, 064512 (2004).
  - [2] E. Pavarini *et al.*, Phys. Rev. Lett **87**, 047003 (2001).
  - [3] Y. Ohta, T. Tohyama and S. Maekawa, Phys. Rev. B **43**,

- 2968 (1991).
- [4] K. McElroy *et al.*, *Science* **309**, 1048 (2005).
- [5] J. A. Slezak *et al.*, *Proc. Natl. Acad. Sci. USA* **105**, 3203 (2008); B. M. Andersen *et al.*, *Phys. Rev. B* **76**, 020507 (2007).
- [6] T. S. Nunner *et al.*, *Phys. Rev. Lett.* **95**, 177003 (2005); M. Mori *et al.*, arXiv:0805.1281.
- [7] J.-X. Zhu, cond-mat/0508646; M. M. Maška *et al.*, *Phys. Rev. Lett.* **99**, 147006 (2007).
- [8] N. N. Kovaleva *et al.*, *Phys. Rev. B* **69**, 54511 (2004).
- [9] (in eV):  $U_{dd} = 8.8$ ,  $U_{pp} = 4.1$ ,  $t_{pd} = 1.2$ ,  $t_{pp} = 0.5$ ,  $\epsilon_d = 0$  and  $\epsilon_p = 2.92$ , where  $U_{pp}$  and  $U_{dd}$  are the on-site Coulomb repulsion for the O 2p and Cu  $3d_{x^2-y^2}$  orbitals,  $t_{pd}$  their overlap, and  $t_{pp}$  is the O 2p-2p overlap integral.
- [10] H. Eskes and J. H. Jefferson, *Phys. Rev. B* **48**, 9788 (1993).
- [11] T. P. Devereaux and R. Hackl, *Rev. Mod. Phys.* **79**, 175 (2007).
- [12] Y. He *et al.*, *Phys. Rev. Lett.* **96**, 197002 (2006).
- [13] H. Eskes and G. Sawatzky, *Phys. Rev. B* **43**, 119 (1991).
- [14] W. A. Harrison, *Elementary Electronic Structure*. World Scientific (2004).
- [15] T. P. Devereaux *et al.*, *Phys. Rev. B* **59**, 14618 (1999).
- [16] A. Macridin *et al.*, *Phys. Rev. Lett.* **97**, 056402 (2006).